Carbon 13 NMR Studies of Saturated Fatty Acids Bound to Bovine Serum Albumin

II. ELECTROSTATIC INTERACTIONS IN INDIVIDUAL FATTY ACID BINDING SITES*

David P. Cistola, Donald M. Small, and James A. Hamilton

From the Biophysics Institute, Housman Medical Research Center, Departments of Medicine and Biochemistry, Boston University School of Medicine, Boston, Massachusetts 02118-2394

^{13}C NMR chemical shift results as a function of pH for a series of carboxyl ^{13}C-enriched saturated fatty acids (8–18 carbons) bound to bovine serum albumin (BSA) are presented. For octanoic acid bound to BSA (6:1, mol/mol), the chemical shift of the only FA carboxyl resonance (designated as peak c), plotted as a function of pH, exhibited a complete sigmoidal titration curve that deviated in shape from a corresponding theoretical Henderson-Hasselbach curve. However, FA carboxyl chemical shift plotted as a function of added HCl yielded a linear titration curve analogous to those obtained for protein-free monomeric fatty acid (FA) in water. The apparent pK of BSA-bound octanoic acid was 4.3 ± 0.2. However, the intrinsic pK (corrected for electrostatic effects resulting from the net positive charge on BSA) was approximately 4.8, a value identical to that obtained for monomeric octanoic acid in water in the absence of protein. For long-chain FA (≥12 carbons) bound to BSA (6:1, mol/mol), chemical shift titration curves for peak c were similar to those obtained for octanoic acid/BSA. However, the four additional FA carboxyl resonances observed (designated as peaks a, b, b', and d) exhibited no change in chemical shift between pH 8 and 3. For $C_{14.0}$·BSA complexes (3:1 and 6:1, mol/mol) peaks b' and a exhibited chemical shift changes between pH 8.8 and 11.5 concomitant with chemical shift changes in the ε-carbon (lysine) resonance. In contrast, peaks c and d exhibited no change and peak b only a slight change in chemical shift over the same pH range. We conclude: (i) the carboxyl groups of bound FA represented by peaks a, b, b', and d were involved in ion pair electrostatic interactions with positively charged amino acyl residues on BSA; (ii) the carboxyl groups of bound FA represented by peak c were not involved in electrostatic interactions with BSA; (iii) the similarity of the titration curves of peak c for BSA-bound octanoic acid and long-chain FA suggested that short-chain and long-chain FA represented by peak c were bound to the same binding site(s) on BSA; (iv) bound FA represented by peaks b' and a (but not d or b) were directly adjacent to BSA lysine residues. We present a model which correlates NMR peaks b, b', and d with the putative locations of three individual high-affinity binding sites in a three-dimensional model of BSA.

In biological systems, free (nonesterified) fatty acids often associate with macromolecules or macromolecular assemblies. For example, FFA[1] in the circulation readily associate with albumin and, under certain physiological or pathological conditions, may associate with lipoproteins, platelets, red blood cells, and neutrophils (Spector and Fletcher, 1978). In order to predict the physical states formed by FFA in these complex systems, the ionization state of the FA carboxyl group must be known (Small, 1968, 1986; Cistola, 1985a, 1985b; 1986). Knowledge of the ionization behavior of bound FFA would aid in understanding not only the mechanism of binding of FFA to a given component of the circulation but also the mechanism of partitioning of FFA between these components and the uptake of FFA by tissue parenchymal cells. However, determination of the ionization behavior of FFA in systems containing multiple ionizable groups and complex macromolecular aggregates is difficult using conventional potentiometric methods and simply assumptions about pK_a values, and more specific methods, such as NMR titration, must be used.

The sensitivity of NMR chemical shifts to the ionization state of chemical groups is well established (Jardetzky and Jardetzky, 1958) and has been extensively utilized to follow the ionization behavior of specific residues in amino acids and proteins (for a review, see Jardetzky and Roberts, 1981). Of the various NMR resonances which exhibit titration shifts, ^{13}C carboxyl resonances are among the most useful because of their large titration shift range and resolution from aliphatic, aromatic, and even carbonyl carbons.

This paper presents ^{13}C NMR titration results for a series of carboxyl ^{13}C-enriched saturated fatty acids (8–18 carbons) bound to bovine serum albumin. NMR chemical shift titration curves at low pH (pH 8–3) indicated differences between high-affinity and low-affinity binding sites with respect to the ionization behavior of bound FA and the involvement of FA/BSA electrostatic interactions in individual FA binding sites. NMR chemical shift titration curves at high pH (pH 7–12) monitored the ionization behavior of lysine ε-ammonium groups and the effects of lysine ionization on the carboxyl

[1] The abbreviations used are: FFA, free nonesterified fatty acid(s); FA, fatty acid(s); BSA, bovine serum albumin; $C_{8.0}$, octanoic acid; $C_{12.0}$, dodecanoic (lauric) acid; $C_{14.0}$, tetradecanoic (myristic) acid; $C_{16.0}$, hexadecanoic (palmitic) acid; $C_{18.0}$, octadecanoic (stearic) acid; δ, chemical shift; Δδ, total change in chemical shift. The use of the abbreviation "FA" or the numerical abbreviations for individual FA compounds is not meant to imply anything about the ionization state of the carboxyl group.
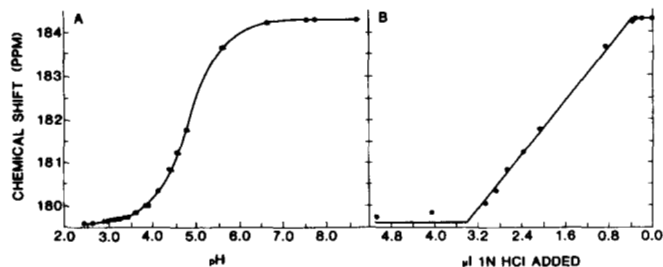
FIG. 1. **^{13}C NMR chemical shift titration curves for 1.6 mM [1-^{13}C]C$_{8.0}$ in water at 40 °C.** *A*, FA carboxyl chemical shift plotted as a function of pH. The *circles* represent experimentally measured values and the *triangles* theoretically calculated (Henderson-Hasselbach) values.[2] *B*, FA carboxyl chemical shift plotted as a function of added 1 N HCl. The *lines* represent a least squares fit of the data points ($r = 0.99$).

chemical shifts of bound FA in individual binding sites. These results permitted further correlation of FA carboxyl resonances with the putative locations of FA binding sites in a three-dimensional model of BSA (Brown and Schockley, 1982; Cistola *et al.*, 1987).

EXPERIMENTAL PROCEDURES

All materials and sample preparation procedures were described in detail in the accompanying paper (Cistola *et al.*, 1987). ^{13}C NMR spectra of FA·BSA complexes (3:1 and 6:1 mole ratio) were recorded as a function of decreasing or increasing pH using instrumentation and techniques described elsewhere (Cistola *et al.*, 1982a, 1987). All FA used in this study were 90% [13]C enriched at the carboxyl carbon position.

RESULTS

As a basis for understanding the more complex NMR titration curves for FA·BSA complexes, NMR titration curves for *protein-free* aqueous [1-^{13}C]C$_{8.0}$ were determined (Fig. 1). The concentration of C$_{8.0}$ used (1.7 mM) was far below the critical micelle concentration of potassium octanoate (400 mM; Mukerjee and Mysels, 1970) and slightly below the solubility limit of fully protonated octanoic acid (2.2 mM; Bell, 1973). The samples exhibited with no visible turbidity or phase separation at any pH value studied. Therefore, C$_{8.0}$ was apparently in monomeric solution throughout the titration.

Two types of plots are shown in Fig. 1. In Fig. 1*A*, the carboxyl chemical shift of C$_{8.0}$ was plotted as a function of pH. The experimental points (*circles*) exhibited a sigmoidal curve and were essentially consistent with the calculated points (*triangles*) for a theoretical Henderson-Hasselbach titration curve.[2] The pK derived from the experimental curve was 4.8 ± 0.1; this value is essentially the same as those

---

[2] The theoretical Henderson-Hasselbach curve was calculated from an NMR version of the Henderson-Hasselbach equation

$$\text{pH} = \text{p}K + \log[(\delta - \delta_{\min})/(\delta_{\max} - \delta)] \quad (1)$$

where $\delta_{\max}$ represents the carboxyl chemical shift for fully ionized FA; $\delta_{\min}$, the chemical shift for fully protonated FA, and δ, the chemical shift at a given pH value. Equation 1 was derived from the more commonly used form of the Henderson-Hasselbach equation

$$\text{pH} = \text{p}K + \log[A^-]/[HA] \quad (2)$$

by equating the following expressions for the fractions of ionized FA present (Cistola *et al.*, 1982a)

$$[A^-]/([HA] + [A]) = (\delta - \delta_{\min})/(\delta_{\max} - \delta_{\min}) \quad (3)$$

and by solving for $[A^-]/[HA]$. $[A^-]$ and $[HA]$ represent the concentrations (or activities) of ionized and protonated FA, respectively. By substituting an experimentally derived pK value into Equation 1, pH values can be calculated for a given δ value.

obtained for shorter-chain carboxylic acids (Cistola *et al.*, 1982a). Fig. 1*B* presents the same chemical shift data plotted as a function of added HCl rather than pH. A linear decrease in carboxyl chemical shift was observed between 0.4 and ~3.2 μl of added HCl with break points at or near the ionization end points. This linear titration curve is analogous to those obtained for water-miscible carboxylic acids in the absence of protein (Cistola *et al.*, 1982a, 1982b).

^{13}C NMR titration curves for C$_{8.0}$·BSA complexes (6:1 mol ratio) as a function of pH and added HCl are shown in Fig. 2, *A* and *B*, respectively. The chemical shifts of the only FA carboxyl peak observed (peak *c*; Cistola *et al.*, 1987) exhibited a complete sigmoidal titration curve (Fig. 2*A*, *circles*) but deviated somewhat from the corresponding theoretical Henderson-Hasselbach curve[2] (Fig. 2*A*, *triangles*). The apparent pK, derived from the experimental curve, was 4.3 ± 0.2. The chemical shift *versus* microliter HCl (Fig. 2*B*) plot exhibited a linear decrease in chemical shift from 35 to 147 μl of added HCl, with break points at the FA ionization end points, and suggested an ionization behavior analogous to protein-free FA monomers in water (Fig. 1*B* and Cistola *et al.*, 1982a).

^{13}C NMR spectra for C$_{14.0}$·BSA complexes (6:1 mole ratio) at selected pH values are shown in Fig. 3. At pH 7.1 (Fig. 3*A*), four partially resolved FA resonances (peaks *a*, *b*, *b'*, and *c*; Cistola *et al.*, 1987) were observed. Below pH 7.1, only peak *c* exhibited chemical shift changes; it shifted upfield with decreasing pH from 181.94 ppm (pH 7.1) to 177.53 ppm (pH 2.9). In contrast, peaks *a*, *b*, and *b'* exhibited no chemical shift changes with decreasing pH. (However, peak *a* decreased in *intensity* below pH 5 and peaks *b* and *b'* decreased in intensity below pH 4.)

Fig. 4 displays chemical shift titration curves for C$_{14.0}$·BSA complexes. For peak *c*, a plot of FA carboxyl chemical shift as a function of pH exhibited a sigmoidal titration curve (Fig. 4*A*, *solid circles*) which deviated from the calculated theoretical Henderson-Hasselbach curve[2] (Fig. 4*A*, *triangles*). The apparent pK, estimated from the experimental curve, was 4.1 ± 0.2. In contrast, peaks *a*, *b*, and *b'* exhibited little or no chemical shift changes with decreasing pH (Fig. 4*A*, *open circles*). Fig. 4*B* shows a linear dependence of the chemical shift of peak *c* on the quantity of added HCl (*solid circles*), with break points at the FA ionization end points, analogous to data for C$_{8.0}$ bound to BSA (Fig. 2*B*) and protein-free C$_{8.0}$ (Fig. 1*B*). In contrast, FA carboxyl peaks *a*, *b*, and *b'* showed little or no chemical shift changes with added HCl (Fig. 4*B*, *open circles*). Thus, with respect to ionization behavior (as followed by ^{13}C NMR), C$_{14.0}$·BSA spectra exhibited two types of FA carboxyl peaks: one type (peak *c*) exhibited complete titration curves similar to those for protein-free FA in water, and the second type (peaks *b*, *b'*, and *a*) exhibited little or no chemical shift change with decreasing pH or added HCl.
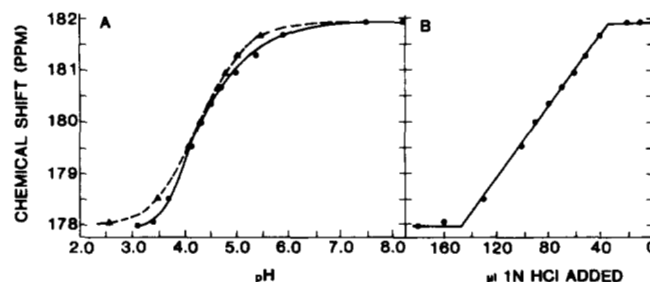

FIG. 2. **^{13}C NMR chemical shift titration curves for [1-^{13}C] C$_{8.0}$·BSA, 6:1 mol ratio, at 35 °C.** *A*, FA carboxyl chemical shift plotted as a function of pH. ●——●, experimentally determined curve; ▲- - -▲, theoretically calculated Henderson-Hasselbach curve.[2] *B*, FA carboxyl chemical shift plotted as a function of added HCl.
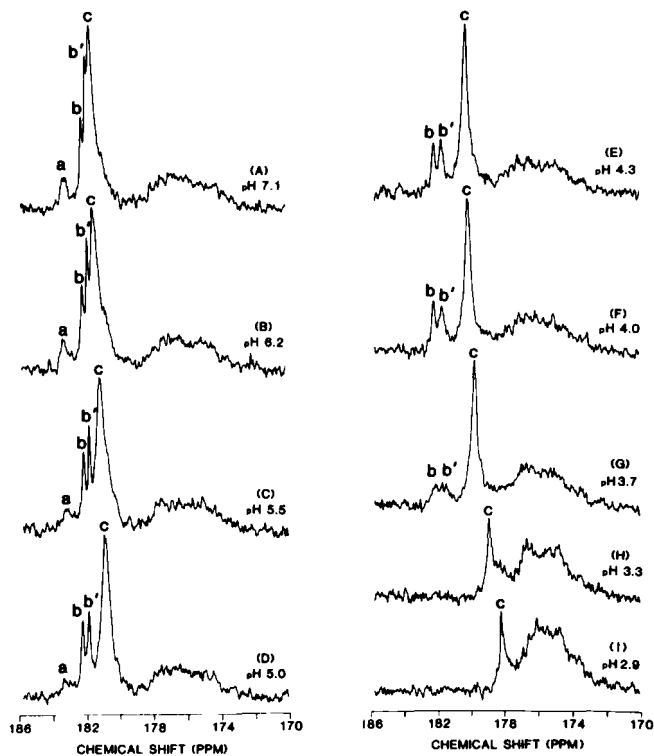
FIG. 3. **Carboxyl/carbonyl region of ^{13}C NMR spectra for $[1\text{-}^{13}C]C_{14.0}\cdot$BSA, 6:1 mol ratio, at different pH values at 34 °C.** Spectra were recorded after 6,000 accumulations with a pulse interval of 2.5 s, 16,384 time domain points, and a spectral width of 10,000 Hz. Identical scaling and processing factors (including 3.0-Hz line broadening) were used for each spectrum. The *lower case letters* above certain peaks indicate specific FA carboxyl resonances with characteristic chemical shifts at pH 7.4 (Cistola *et al.*, 1987).
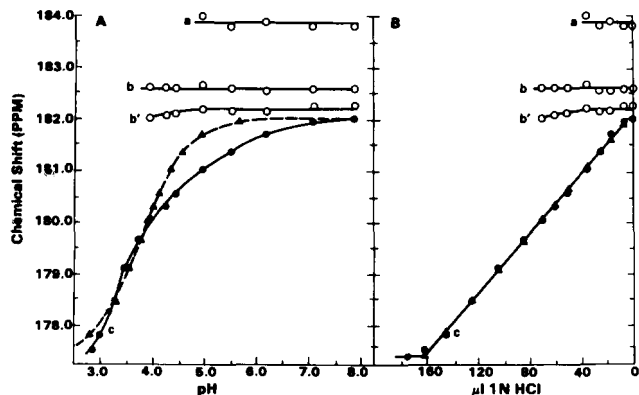

FIG. 4. **^{13}C NMR chemical shift titration curves for $[1\text{-}^{13}C]$ $C_{14.0}\cdot$BSA, 6:1 mol ratio, at 35 °C.** O———O, experimentally determined curves for peaks *a, b,* and *b'* (see Fig. 3); ●———●, experimentally determined curves for peak *c* (Fig. 3); ▲– – –▲, theoretically calculated Henderson-Hasselbach curves for peak *c*.[2] The experimental data points were derived from the NMR spectra shown in Fig. 3 as well as other spectra not shown. *A*, FA carboxyl chemical shifts plotted as a function of pH. *B*, FA carboxyl chemical shifts plotted as a function of added HCl.

^{13}C NMR spectra (not shown) of $C_{12.0}\cdot$BSA complexes (6:1 mole ratio) obtained at pH values between 8.0 and 2.8 were very similar to those for $C_{14.0}\cdot$BSA complexes. The corresponding NMR chemical shift titration curves for $C_{12.0}\cdot$BSA complexes are shown in Fig. 5. One FA carboxyl peak (*c*) exhibited complete titration curves with decreasing pH (Fig. 5*A*) or added HCl (Fig. 5*B*). In contrast, peaks *b* and *b'* exhibited no change in chemical shift over this pH range. A
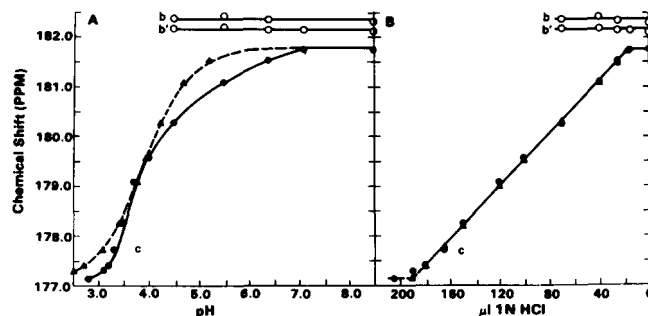

FIG. 5. **^{13}C NMR chemical shift titration curves for $[1\text{-}^{13}C]$ $C_{12.0}\cdot$BSA, 6:1 mol ratio, at 35 °C.** Symbols are defined as described in the legend to Fig. 4. *A*, FA carboxyl chemical shifts as a function of pH. *B*, FA carboxyl chemical shifts plotted as a function of added HCl.
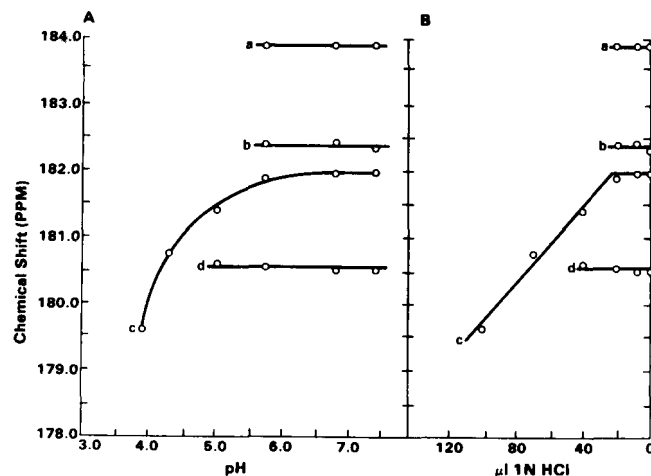

FIG. 6. **^{13}C NMR chemical shift titration curves for $[1\text{-}^{13}C]$ $C_{16.0}\cdot$BSA, 6:1 mol ratio, at 35 °C.** *A*, FA carboxyl chemical shift plotted as a function of pH. *B*, FA carboxyl chemical shift plotted as a function of added HCl. The FA carboxyl peaks became undetectable below pH 4.0 (above 100 µl of HCl).

plot of chemical shift as a function of pH for peak *c* (Fig. 5*A, solid circles*) was sigmoidal with an apparent pK_a of 4.1 ± 0.2 but deviated from the calculated Henderson-Hasselbach curve (Fig. 5*A, triangles*). A plot of chemical shift as a function of added HCl for peak *c* (Fig. 5*B, solid circles*) was linear ($r = -0.99$) with break points at the FA ionization end points, analogous to data for $C_{14.0}\cdot$BSA (peak *c*; Fig. 3), $C_{8.0}\cdot$BSA (peak *c*, Fig. 2), and protein-free $C_{8.0}$ (Fig. 1).

^{13}C NMR spectra for $C_{16.0}\cdot$BSA and $C_{18.0}\cdot$BSA complexes (not shown) were similar to those for $C_{14.0}\cdot$BSA and $C_{12.0}\cdot$ BSA except for one major difference: for $C_{16.0}\cdot$BSA and $C_{18.0}\cdot$ BSA, peak *c* became undetectable below pH 3.9. Therefore, complete titration curves for peak *c* could not be generated. However, a partial titration curve for $C_{16.0}\cdot$BSA (peak *c*) is shown in Fig. 6. As with $C_{14.0}\cdot$BSA and $C_{12.0}\cdot$BSA, only peak *c* exhibited chemical shift changes with decreasing pH or added HCl for $C_{16.0}\cdot$BSA (Fig. 6) and $C_{18.0}\cdot$BSA (not shown). Peaks *a, b,* and *d* yielded no chemical shift changes with decreasing pH or added HCl.

Two $C_{14.0}\cdot$BSA samples (3:1 and 6:1 mole ratio) were titrated with 1.0 N KOH from pH 7.4 to 11.9. At 3:1 mole ratio, essentially all of the $C_{14.0}$ was bound to the three high-affinity binding sites on BSA (represented by peaks *b, b',* and *d*; Cistola *et al.*, 1987). The chemical shift of the ϵ-carbon of lysine increased with increasing pH beginning at pH 8.8 concomitant with a decrease in chemical shift of FA carboxyl peak *b'* above 8.8 (Fig. 7). FA carboxyl peak *b* exhibited a
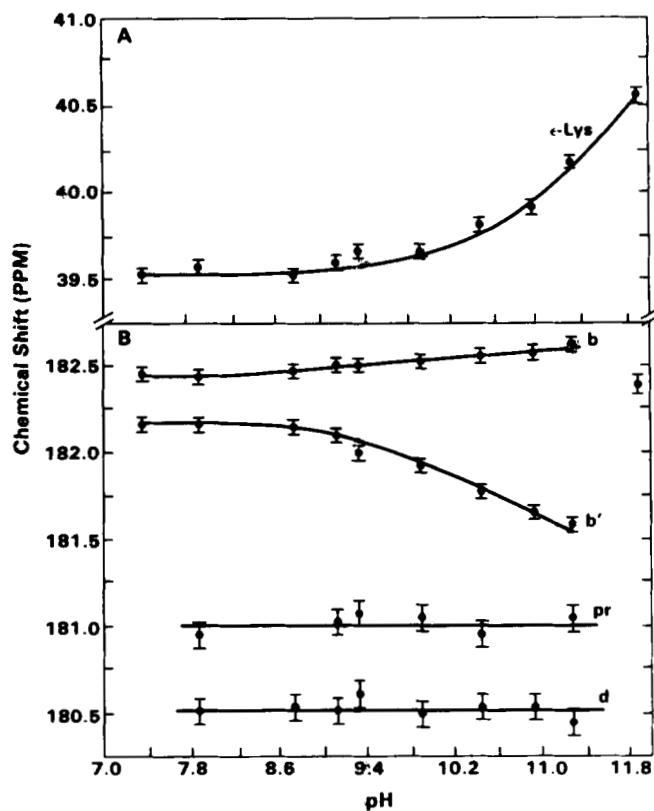
FIG. 7. ^{13}C NMR chemical shift titration curves at high pH for [1-^{13}C]C$_{14.0}$·BSA, 3:1 mol ratio, at 34 °C. The NMR sample was titrated with 1 N KOH from pH 7.4 to 11.9. External tetramethylsilane in a capillary was used as a chemical shift reference. *Vertical error bars* represent estimated uncertainties in chemical shift determinations. *A*, chemical shift of ε-carbon (lysine) resonance as a function of pH. *B*, carboxyl chemical shift of FA carboxyl peaks *b*, *b'*, and *d* (*cf.* Fig. 3) and BSA glutamate carboxyl peak *pr* (Cistola *et al.,* 1987) as a function of pH.

small but significant increase with increasing pH, and peaks *d* and *pr* (glutamate carboxyl) demonstrated no chemical shift change with increasing pH. In spectra of 6:1 mole ratio complexes, in which peaks *a* and *c* were observed (in addition to peaks *b*, *b'*, and *d*), the chemical shift of peak *a* decreased above pH 8.8 (data not shown) in a manner similar to peak *b'* (Fig. 7).

DISCUSSION

As shown in the accompanying paper (Cistola *et al.,* 1987), ^{13}C NMR spectra of ^{13}C-enriched saturated long-chain FA bound to BSA at pH 7.4 contained multiple FA carboxyl resonances corresponding to multiple FA binding sites. Three of these resonances (*b*, *b'*, and *d*) were correlated with the three high-affinity long-chain FA binding sites deduced from Scatchard analyses of binding data (Spector *et al.,* 1969) and from Brown and Schockley's (1982) three-dimensional model of BSA. In the latter model, NMR peaks *b*, *b'*, and *d* apparently represented long-chain FA bound to binding sites 1-C, 3-C, and 2-C, respectively (Cistola *et al.,* 1987). In contrast, the FA carboxyl resonance labeled *c* was correlated with the nonspecific sites such as these located in subdomains 1-AB, 2-AB, and/or 3-AB of Brown and Schockley's model. Peak *a* represented a low-affinity (secondary) long-chain FA binding site in subdomain 2-AB. In this study, the ionization behavior of [^{13}C]carboxyl-enriched FA bound to BSA was determined by ^{13}C NMR spectroscopy in order to assess whether ion pair interactions occur between FA carboxyl groups and neighbor-

ing protein residues in individual FA binding sites.

Based on studies of spin-label FA analogues or detergents bound to albumin (Morrisett *et al.,* 1975), it has been suggested that hydrophobic interactions are the dominant mechanism by which FA bind to albumin (Spector, 1975). For alkyl sulfate detergents, binding affinities for albumin increase as the alkyl chain length increases (Karush and Sonnenberg, 1949). Aminoazobenzene, an uncharged derivative of methyl orange, binds nearly as well as methyl orange itself (Klotz and Ayers, 1952). For organic anions, there is a large positive entropy change for the first mole bound but only a small enthalpy change (Klotz and Urquhart, 1949), suggesting that binding is primarily an entropy effect resulting from a release of water when the ligand protein complex forms (Spector, 1975).

However, there is also evidence that electrostatics play at least a minor role in ligand/albumin interactions. Based on indirect evidence, it has long been thought that FA bound to albumin are anionic at pH 7.4 (Ballou *et al.,* 1945). This conclusion was directly confirmed by the ^{13}C NMR titration curves presented previously for oleic acid (Parks *et al.,* 1983) and myristic acid (Hamilton *et al.,* 1984) along with curves presented in this study, at least for bound FA represented by NMR peak *c*. Furthermore, the relative absorption of an anionic dye (methyl orange) bound to BSA was altered over a pH range in which the ε-ammonium group of lysine residues would be expected to ionize (Klotz and Walker, 1947). In addition, studies using spin-label analogues of fatty acids have shown that methyl ester analogues bind with lower affinity than carboxylate ion analogues (Morrisett *et al.,* 1975). However, few studies have utilized native FA, and little information is available about the relative importance of hydrophobic and electrostatic interactions in *individual* binding sites. The NMR titration results presented in this study address both of these concerns.

In titration from pH 8 to pH 3 (Figs. 2–6), FA bound to BSA exhibited two types of ionization behavior. The first type (peak *c* only) was characterized by NMR titration curves analogous to those obtained for protein-free monomeric FA in water. In contrast, the second type of ionization behavior (peaks *a*, *b*, *b'*, and *d*) was characterized by no changes in FA carboxyl chemical shift with decreasing pH.

The ionization behavior of peak *c* was analogous to protein-free FA monomers in water according to three criteria: Δδ values, apparent p*K* values, and the shape of NMR titration curves. First, the Δδ value for FA·BSA complexes (except C$_{8.0}$·BSA) was 4.7 ppm, identical to that for aqueous protein-free C$_{8.0}$ (Fig. 1) and aqueous short-chain carboxylic acids (Cistola *et al.,* 1982a). Second, the experimentally determined apparent p*K* values of FA bound to BSA (p*K* = 4.1–4.3) were somewhat lower than values obtained for protein-free monomeric FA in water (p*K* = 4.7–4.9; Fig. 1 and Cistola *et al.,* 1982a). However, after correction of these pK_a values for electrostatic effects[3] resulting from the net positive charge on

---

[3] Intrinsic p*K* values (pK_{int}) for FA (peak *c*) bound to BSA were estimated using the equation

$$pK_{int} = pH + 0.868wZ$$

where the term $0.868wZ$ takes into account the electrostatic interactions between the net charge (*Z*) of BSA at a given pH value and dissociating hydrogen ions (Tanford *et al.,* 1955). Values for the electrostatic interaction factor (*w*) can be determined empirically or calculated from an equation derived from Debye-Hückel theory (Tanford *et al.,* 1955). We used values of 0.052 and 0.065, respectively, in these calculations. The net charge *Z* was determined from the equation

BSA at pH 4.1, the resulting intrinsic pK values (4.5–4.8) were essentially the same as values for protein-free monomeric FA in water. Third, the shape of NMR chemical shift titration curves for peak c were very similar to those obtained for aqueous protein-free FA (Fig. 1). Although plots of chemical shifts (peak c) as a function of pH yielded titration curves which deviated from idealized Henderson-Hasselbach ionization behavior, chemical shift *versus* added HCl exhibited a linear decrease analogous to that obtained for protein-free monomeric FA in water (Fig. 1 and Cistola *et al.*, 1982a). Thus, changes in FA chemical shifts were sensitive only to changes in FA ionization state, rather than the carboxyl group's molecular environment (*e.g.* alterations caused by BSA conformational changes). The latter would have been characterized by a nonlinearity, a change in slope of chemical shift titration curves, or a $\Delta\delta$ unequal to the expected value. The linear plots also suggested that the deviation from Henderson-Hasselbach ionization behavior shown in Figs. 2A, 4A, and 5A arose in the pH term, not the chemical shift term, of Equation 1.[2] The most likely explanation for anomalous pH values in the carboxyl ionization region is the unmasking of BSA carboxylate groups during the N-F conformational transition below pH 5 (Foster, 1977). Apparently, the N-F transition does not give rise to anomalous FA carboxyl *chemical shift* values for the bound FA represented by peak c. However, this transition does result in a loss of *intensity* of FA carboxyl peaks (Fig. 3).[4]

The similarities between the ionization behavior of FA bound to BSA (peak c) and the ionization behavior of protein-free FA monomers in water suggested that the FA carboxyl groups of bound FA represented by peak c were freely accessible to the aqueous solvent and, therefore, free of specific electrostatic interactions with side chain residues on BSA. In contrast, the *lack* of NMR titration shifts for bound FA represented by peaks a, b, b', and d suggested that FA carboxyl groups in these binding sites were solvent-inaccessible and were probably involved in ion pair electrostatic interactions with basic amino acid residues that line the mouths of several of the putative FA binding sites on BSA (Brown and Schockley, 1982).

In an attempt to determine which positively charged BSA side chain residues interact with the carboxylate groups of bound FA (represented by peaks a, b, b', and d), $C_{14.0}\cdot$BSA complexes (3:1 and 6:1 mole ratio) were titrated with KOH from pH 7.4 to pH 12.2. For 3:1 mole ratio complexes (Fig. 7), peak b' and the ϵ-carbon resonance (lysine) exhibited substantial chemical shift changes between pH 8.8 and 11.3. In contrast, peak b exhibited only slight chemical shift changes and peaks d and pr no chemical shift changes between pH 8.8 and 11.3. There are three possible explanations for these results. (i) $C_{14.0}\cdot$BSA may have undergone gross conformational change(s) over this pH range which could have altered the local molecular environment around lysine ϵ-carbons and FA carboxyl carbons. Spectral changes characteristic of protein unfolding and/or peptide cleavage did occur at pH values >11.5. However, these changes did not occur between pH 8.8 and 11.3. Alternatively, a localized change in BSA structure might have affected only certain portions of the molecule and, hence, only certain of the observed NMR

resonances. Since conformational changes have not been detected over this pH range (Foster, 1977), this explanation is unlikely. (ii) FA carboxyl ionization may have given rise to the observed chemical shift changes in peak b' and also affected nearby lysine residues. However, the pK values of carboxyl groups are generally much lower than the pH range being considered here. In addition, the chemical shift of peak b' exhibited a much smaller $\Delta\delta$ value than, and changed in the opposite direction of, that expected for FA carboxyl ionization. Therefore, this second explanation is highly unlikely.

The most plausible explanation for changes in the molecular environment of the FA carboxyl (between pH 8.8 and 11.3) is ionization of a basic amino acid residue such as lysine, tyrosine, or arginine. Arginine guanidinium groups have extremely high intrinsic pK values (>13) in small molecules such as guanidine and substituted guanidines (Cohn and Edsall, 1943; Neivelt *et al.*, 1951) and pK values >12 in proteins such as lysozyme and BSA (Tanford *et al.*, 1955). For tyrosine phenolic hydroxyl groups in BSA, the experimentally observed pH value at the ionization midpoint (uncorrected for electrostatic effects resulting from the net charge of the protein) was 11.5 (Tanford and Roberts, 1952; Decker and Foster, 1967). Since the observed effect on FA occurs between pH 8.8 and 11.5, these amino acids probably would not be responsible. In contrast, ϵ-ammonium groups in BSA have a pH midpoint for lysine ionization of approximately 10.7 (Tanford *et al.*, 1955). Chemical shift changes in the ϵ-carbon of lysine occurred over this pH range (Fig. 7A). Therefore, we conclude that lysine ionization occurs between pH 8.8 and 11.5 and affects the chemical environment of adjacent FA carboxyl groups represented by peak b' (Fig. 7).

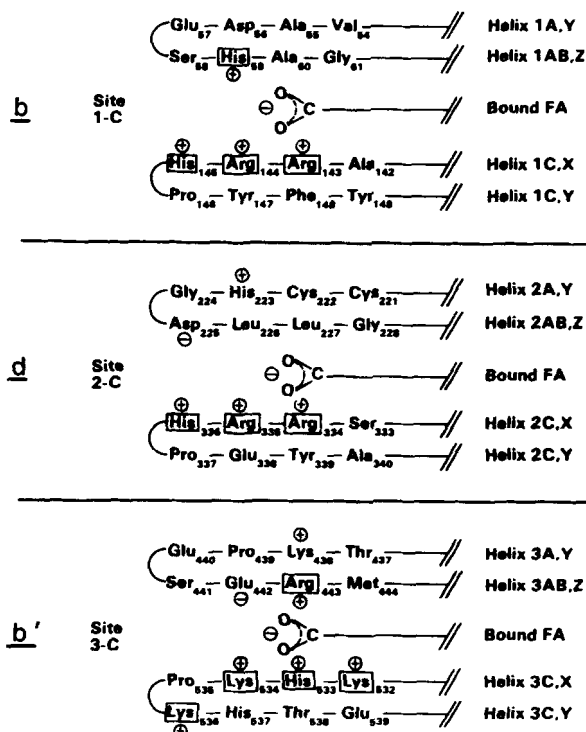Taken together, the titration results for different FA allow

FIG. 8. Schematic diagram depicting putative locations of bound FA molecules in three high-affinity long-chain FA binding sites on BSA. The nomenclature used for α-helices and the amino acid sequences in the putative binding sites are from Brown and Schockley (1982). We propose that the FA represented by NMR peak b' is bound to site 3-C, the FA represented by peak b at site 1-C, and the FA represented by peak d at site 2-C (see also Cistola *et al.*, 1987).

$$Z = 96 - r - \psi_{cl}$$

where r was taken to be 80 and ψ_{cl} (the moles of bound chloride ions/mol of BSA) 6 (Carr, 1953; Steinhardt and Reynolds, 1969). Final estimated pK_{int} values were 4.6–4.7 for long-chain FA·BSA complexes and 4.8–4.9 for $C_{8.0}\cdot$BSA complexes.

[4] The effect of BSA conformational changes on ^{13}C NMR results will be addressed in detail in a future paper.

DOCKET ALARM

Explore Litigation Insights

Docket Alarm provides insights to develop a more informed litigation strategy and the peace of mind of knowing you're on top of things.

Real-Time Litigation Alerts

Keep your litigation team up-to-date with **real-time alerts** and advanced team management tools built for the enterprise, all while greatly reducing PACER spend.

Our comprehensive service means we can handle Federal, State, and Administrative courts across the country.

Advanced Docket Research

With over 230 million records, Docket Alarm's cloud-native docket research platform finds what other services can't. Coverage includes Federal, State, plus PTAB, TTAB, ITC and NLRB decisions, all in one place.

Identify arguments that have been successful in the past with full text, pinpoint searching. Link to case law cited within any court document via Fastcase.

Analytics At Your Fingertips

Learn what happened the last time a particular judge, opposing counsel or company faced cases similar to yours.

Advanced out-of-the-box PTAB and TTAB analytics are always at your fingertips.

API

Docket Alarm offers a powerful API (application programming interface) to developers that want to integrate case filings into their apps.

LAW FIRMS
Build custom dashboards for your attorneys and clients with live data direct from the court.

Automate many repetitive legal tasks like conflict checks, document management, and marketing.

FINANCIAL INSTITUTIONS
Litigation and bankruptcy checks for companies and debtors.

E-DISCOVERY AND LEGAL VENDORS
Sync your system to PACER to automate legal marketing.

fastcase®
Smarter legal research.